*Inorg. Chem.* **2006**, *45*, 8895–8901

# Cyano-Bridged Pentanuclear $Fe^{III}_3M^{II}_2$ (M = Ni, Co, Fe) Clusters: Synthesis, Structures, and Magnetic Properties

**Zhi-Guo Gu, Qiao-Fang Yang, Wei Liu, You Song, Yi-Zhi Li, Jing-Lin Zuo,* and Xiao-Zeng You**

*Coordination Chemistry Institute and the State Key Laboratory of Coordination Chemistry, School of Chemistry and Chemical Engineering, Nanjing University, Nanjing 210093, P. R. China*

Received May 6, 2006

The reactions of $[M^{II}(Tpm^{Me})(H_2O)_3]^{2+}$ (M = Ni, Co, Fe; $Tpm^{Me}$ = tris(3,5-dimethyl-1-pyrazoyl)methane) with $[Bu_4N][(Tp)Fe^{III}(CN)_3]$ ($Bu_4N^+$ = tetrabutylammonium cation; Tp = tris(pyrazolyl)hydroborate) in MeCN–$Et_2O$ afford three pentanuclear cyano-bridged clusters, $[(Tp)_3(Tpm^{Me})_2Fe^{III}_3M^{II}_2(CN)_9]ClO_4\cdot 15H_2O$ (M = Ni, **1**; M = Co, **2**) and $[(Tp)_3(Tpm^{Me})_2Fe^{III}_3Fe^{II}_2(CN)_9]BF_4\cdot 15H_2O$ (**3**). Single-crystal X-ray analyses reveal that they show the same trigonal bipyramidal structure featuring a $D_{3h}$-symmetry core, in which two opposing $Tpm^{Me}$-ligated $M^{II}$ ions situated in the two apical positions are linked through cyanide bridges to an equatorial triangle of three Tp-ligated $Fe^{III}$ ($S = {}^1/_2$) centers. Magnetic studies for complex **1** show ferromagnetic coupling giving an $S = 7/2$ ground state and an appreciable magnetic anisotropy with a negative $D_{7/2}$ value equal to $-0.79$ cm$^{-1}$. Complex **2** shows zero-field splitting parameters deducted from the magnetization data with $D = -1.33$ cm$^{-1}$ and $g = 2.81$. Antiferromagnetic interaction was observed in complex **3**.

## Introduction

Molecules possessing a high-spin ground state with negative axial zero-field splitting, commonly referred to as single-molecule magnets (SMMs), are attracting a great deal of interest because of their unique physical properties and possible applications in quantum computing and magnetic refrigeration.[1] The majority of SMMs reported by far are transition metal−oxo clusters.[2−5] Cyanide, as the efficient linear bridge mediating the magnetic interaction between two metal ions, is an alternative bridging ligand for preparing high-spin clusters.[6] One of the approaches to synthesize metal−cyanide clusters is the reaction of hexacyanometalate[7] or octacyanometalate[8] with paramagnetic metal ions or cationic complexes, but high-nuclearity complexes are difficult to obtain from them since extended networks are

* To whom correspondence should be addressed. E-mail: zuojl@nju.edu.cn. Fax: +86-25-83314502.

(1) (a) Christou, G.; Gatteschi, D.; Hendrickson, D. N.; Sessoli, R. *MRS Bull.* **2000**, *25*, 66. (b) Gatteschi, D.; Sessoli, R. *Angew. Chem., Int. Ed.* **2003**, *42*, 268.

(2) (a) Sessoli, R.; Gatteschi, D.; Caneschi, A.; Novak, M. A. *Nature (London)* **1993**, *365*, 141. (b) Aubin, S. M. J.; Wemple, M. W.; Adams, D. M.; Tsai, H. L.; Christou, G.; Hendrickson, D. N. *J. Am. Chem. Soc.* **1996**, *118*, 7746. (c) Boskovic, C.; Bircher, R.; Tregenna-Piggott, P. L. W.; Güdel, H. U.; Paulsen, C.; Wernsdorfer, W.; Barra, A.-L.; Khatsko, E.; Neels, A.; Stoeckli-Evans, H. *J. Am. Chem. Soc.* **2003**, *125*, 14046. (d) Miyasaka, H.; Clérac, R.; Wernsdorfer, W.; Lecren, L.; Bonhomme, C.; Sugiura, K.; Yamashita, M. *Angew. Chem., Int. Ed.* **2004**, *43*, 2801. (e) Murugesu, M.; Habrych, M.; Wernsdorfer, W.; Abboud, K. A.; Christou, G. *J. Am. Chem. Soc.* **2004**, *126*, 4766. (f) Stamatatos, T. C.; Foguet-Albiol, D.; Stoumpos, C. C.; Raptopoulou, C. P.; Terzis, A.; Wernsdorfer, W.; Perlepes, S. P.; Christou, G. *J. Am. Chem. Soc.* **2005**, *127*, 15380.

(3) (a) Oshio, H.; Hoshino, N.; Ito, T. *J. Am. Chem. Soc.* **2000**, *122*, 12602. (b) Oshio, H.; Hoshino, N.; Ito, T.; Nakano, M. *J. Am. Chem. Soc.* **2004**, *126*, 8805. (c) Accorsi, S.; Barra, A.-L.; Caneschi, A.; Chastanet, G.; Cornia, A.; Fabretti, A. C.; Gatteschi, D.; Mortalo, C.; Olivieri, E.; Parenti, F.; Rosa, P.; Sessoli, R.; Sorace, L.; Wernsdorfer, W.; Zobbi, L. *J. Am. Chem. Soc.* **2006**, *128*, 4742. (d) Andres, H.; Basler, R.; Blake, A. J.; Cadiou, C.; Chaboussant, G.; Grant, C. M.; Gudel, H.-U.; Murrie, M.; Parsons, S.; Paulsen, C.; Semadini, F.; Villar, V.; Wernsdorfer, W.; Winpenny, R. E. P. *Chem.*—Eur. J. **2002**, *8*, 4867. (e) Yang, E.-C.; Wernsdorfer, W.; Zakharov, L. N.; Karaki, Y.; Yamaguchi, A.; Isidro, R. M.; Lu, G.-D.; Wilson, S. A.; Rheingold, A. L.; Ishimoto, H.; Hendrickson, D. N. *Inorg. Chem.* **2006**, *45*, 529.

(4) (a) Castro, S. L.; Sun, Z.; Grant, C. M.; Bollinger, J. C.; Hendrickson, D. N.; Christou, G. *J. Am. Chem. Soc.* **1998**, *120*, 2365. (b) Yang, E.; Hendrickson, D. N.; Wernsdorfer, W.; Nakano, M.; Zakharov, L. N.; Sommer, R. D.; Rheingold, A. L.; Ledezma-Gairaud, M.; Christou, G. *J. Appl. Phys.* **2002**, *91*, 7382. (c) Karasawa, S.; Zhou, G.; Morikawa, H.; Koga, N. *J. Am. Chem. Soc.* **2003**, *125*, 13676. (d) Tang, J. K.; Hewitt, I.; Madhu, N. T.; Chastanet, G.; Wernsdorfer, W.; Anson, C. E.; Benelli, C.; Sessoli, R.; Powell, A. K. *Angew. Chem., Int. Ed.* **2006**, *45*, 1729. (e) Accorsi, S.; Barra, A.-L.; Caneschi, A.; Chastanet, G.; Cornia, A.; Fabretti, A. C.; Gatteschi, D.; Mortalo, C.; Olivieri, E.; Parenti, F.; Rosa, P.; Sessoli, R.; Sorace, L.; Wernsdorfer, W.; Zobbi, L. *J. Am. Chem. Soc.* **2006**, *128*, 4742.

(5) (a) Osa, S.; Kido, T.; Matsumoto, N.; Re, N.; Pochaba, A.; Mrozinski, J. *J. Am. Chem. Soc.* **2004**, *126*, 420. (b) Zaleski, C. M.; Depperman, E. C.; Kampf, J. W.; Kirk, M. L.; Pecoraro, V. L. *Angew.* Chem., *Int. Ed.* **2004**, *43*, 3912. (c) Oshio, H.; Nihei, M.; Koizumi, S.; Shiga, T.; Nojiri, H.; Nakano, M.; Shirakawa, N.; Akatsu, M. *J. Am. Chem. Soc.* **2005**, *127*, 4568. (d) Mori, F.; Nyui, T.; Ishida, T.; Nogami, T.; Choi, K.-Y.; Nojiri, H. *J. Am. Chem. Soc.* **2006**, *128*, 1440.

10.1021/ic060772h CCC: $33.50 
Published on Web 10/07/2006

favored for kinetic reasons in most cases. Recently, a new synthetic strategy for achieving cyanide-bridged molecules with higher nuclearities was reported by using *fac*-$LM(CN)_3$ as building blocks. The introduction of multidentate blocking ligands can inhibit the growth of an extended solid and promote the construction of multinuclear clusters instead of polymers.[9−11] In our previous work, we have employed the tricyanometalate precursor, $(Bu_4N)[(Tp)Fe(CN)_3]$ ($Bu_4N^+$ = tetrabutylammonium cation; Tp = tris(pyrazolyl)hydroborate), to prepare a face-centered cubic cluster $[(Tp)_8(H_2O)_6Cu^{II}_6Fe^{III}_8(CN)_{24}]^{4+}$ exhibiting SMM-type behavior.[12] Very recently, we used a tridentate blocking ligand $Me_3tacn$ (*N*,*N*′,*N*″-trimethyl-1,4,7-triazacyclononane) on the $Cu^{II}$ centers in above system to generate a trigonal bipyramidal cluster, $[Tp_2(Me_3tacn)_3Cu_3Fe_2(CN)_6]^{4+}$, in which the reduced symmetry affords a significantly increased anisotropy barrier.[13] To further stabilize high-nuclearity complexes, in this paper, we choose the complex $[M(Tpm^{Me})(H_2O)_3]^{2+}$ (M = $Ni^{2+}$, $Co^{2+}$, $Fe^{2+}$; $Tpm^{Me}$ = tris(3,5-dimethyl-1-pyrazoyl)-methane) as a "metal" (Chart 1), in which the three solvated molecules are labile and the bulky ligand environment precludes the formation of extended arrays. Therefore, the reaction should be under thermodynamic control.

**Chart 1**

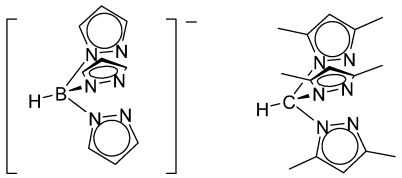

Tp $Tpm^{Me}$

The $Tpm^{Me}$ was chosen to design cationic complexes for two reasons: (i) $Tpm^{Me}$ is a scorpionate ligand bearing a $C_3$ axis, and the corresponding cationic complexes have three potentially available sites to coordinate to tricyanometalate. (ii) The formed cationic complexes of $Tpm^{Me}$ are more soluble in organic solvents compared to the analogues of Tpm (Tpm = tris(pyrazoyl)methane).

$$2[M(Tpm^{Me})(H_2O)_3]^{2+} + 3[(Tp)Fe(CN)_3]^- \rightarrow [(Tp)_3(Tpm^{Me})_2M_2Fe_3(CN)_9]^+ \quad (1)$$

Using this method, reaction 1 carried out in acetonitrile produced three new pentanuclear cyano-bridged clusters: $[(Tp)_3(Tpm^{Me})_2Ni_2Fe_3(CN)_9]ClO_4\cdot 15H_2O$ (**1**); $[(Tp)_3(Tpm^{Me})_2Co_2Fe_3(CN)_9]ClO_4\cdot 15H_2O$ (**2**); $[(Tp)_3(Tpm^{Me})_2Fe_5(CN)_9]BF_4\cdot 15H_2O$ (**3**). Herein, we report the synthesis and magnetic properties of these three clusters. In the comparatively simple isostructural clusters, the introduction of different transition metal ions affords different magnetic properties, which may provide an effective method to investigate the magneto−structure correlation.

## Experimental Section

**Synthesis.** All chemicals were reagent grade and used as received. $(Bu_4N)[(Tp)Fe(CN)_3]$[14] and $[Fe(Tpm^{Me})(H_2O)_3](BF_4)_2$[15a] were prepared according to the literature method.

**Caution!** The cyanides are very toxic and should be handled in small quantities and with great caution.

**Preparation of Complex $[(Tp)_3(Tpm^{Me})_2Ni_2Fe_3(CN)_9]ClO_4\cdot 15H_2O$ (1).** An acetonitrile solution (2 mL) of $Ni(ClO_4)_2\cdot 6H_2O$ (36.5 mg, 0.10 mmol) was added dropwise to an acetonitrile solution (2 mL) of $HC(3,5\text{-}Me_2pz)_3$ (29 mg, 0.10 mmol). To this reaction mixture, $(Bu_4N)[(Tp)Fe(CN)_3]$ (88 mg, 0.15 mmol) in 3 mL of


(6) (a) Marvaud, V.; Decroix, C.; Scuiller, A.; Guyard-Duhayon, C.; Vaissermann, J.; Gonnet, F.; Verdaguer, M. *Chem.*—Eur. J. **2003**, *9*, 1677. (b) Marvaud, V.; Decroix, C.; Scuiller, A.; Tuyèras, F.; Guyard-Duhayon, C.; Vaissermann, J.; Marrot, J.; Gonnet, F.; Verdaguer, M. *Chem.*—Eur. J. **2003**, *9*, 1692. (c) Beltran, L. M. C.; Long, J. R. *Acc. Chem. Res.* **2005**, *38*, 325.

(7) (a) Scuiller, A.; Mallah, T.; Verdaguer, M.; Nivorozkhin, A.; Tholence, J. L.; Veillet, P. *New J. Chem.* **1996**, *20*, 1. (b) Vostrikova, K. E.; Luneau, D.; Wernsdorfer, W.; Rey, P.; Verdaguer, M. *J. Am. Chem. Soc.* **2000**, *122*, 718. (c) Rogez, G.; Marvilliers, A.; Rivière, E.; Audière, J.-P.; Lloret, F.; Varret, F.; Goujon, A.; Mendenez, N.; Girerd, J.-J.; Mallah, T. *Angew. Chem., Int. Ed.* **2000**, *39*, 2885. (d) Berlinguette, C. P.; Vaughn, D.; Cañada-Vilalta, C.; Galán-Mascarós, J. R.; Dunbar, K. R. *Angew. Chem., Int. Ed.* **2003**, *42*, 1523. (e) Ferbinteanu, M.; Miyasaka, H.; Wernsdorfer, W.; Nakata, K.; Sugiura, K.; Yamashita, M.; Coulon, C.; Clérac, R. *J. Am. Chem. Soc.* **2005**, *127*, 3090. (f) Rebilly J. N.; Catala L.; Rivière E.; Guillot R.; Wernsdorf W.; Mallah T. *Chem. Commun.* **2006**, 735.

(8) (a) Larionova, J.; Gross, M.; Pilkington, M.; Andres, H.; Stoeckli-Evans, H.; Güdel, H. U.; Decurtins, S. *Angew. Chem., Int. Ed.* **2000**, *39*, 1605. (b) Zhuang, J. Z.; Seino, H.; Mizobe, Y.; Hidai, M.; Fujishima, A.; Ohkoshi, S.; Hashimoto, K. *J. Am. Chem. Soc.* **2000**, *122*, 2952. (c) Song, Y.; Zhang, P.; Ren, X. M.; Shen, X. F.; Li, Y. Z.; You X. Z. *J. Am. Chem. Soc.* **2005**, *127*, 3708. (d) Ruiz, E.; Rajaraman, G.; Alvarez, S.; Gillon, B.; Stride, J.; Clérac, R.; Larionova, J.; Decurtins S. *Angew. Chem., Int. Ed.* **2005**, *44*, 2711.

(9) (a) Shores, M. P.; Sokol, J. J.; Long, J. R. *J. Am. Chem. Soc.* **2002**, *124*, 2279. (b) Sokol, J. J.; Hee, A. G.; Long, J. R. *J. Am. Chem. Soc.* **2002**, *124*, 7656. (c) Berseth, P. A.; Sokol, J. J.; Shores, M. P.; Heinrich, J. L.; Long, J. R. *J. Am. Chem. Soc.* **2000**, *122*, 9655. (d) Heinrich, J. L.; Sokol, J. J.; Hee, A. G.; Long, J. R. *J. Solid State Chem.* **2001**, *159*, 293. (e) Sokol, J. J.; Shores, M. P.; Long, J. R. *Angew. Chem., Int. Ed.* **2001**, *40*, 236. (f) Sokol, J. J.; Shores, M. P.; Long, J. R. *Inorg. Chem.* **2002**, *41*, 3052. (g) Yang, J. Y.; Shores, M. P.; Sokol, J. J.; Long, J. R. *Inorg.* Chem. **2003**, *42*, 1403. (h) Heinrich, J. L.; Berseth, P. A.; Long, J. R. *Chem. Commun.* **1998**, 1231.

(10) (a) Schelter, E. J.; Prosvirin, A. V.; Dunbar, K. R. *J. Am. Chem. Soc.* **2004**, *126*, 15004. (b) Dunbar, K. R.; Schelter, E. J.; Palii, A. V.; Ostrovsky, S. M.; Mirovitskii, V. Y.; Hudson, J. M.; Omary, M. A.; Klokishner, S. I.; Tsukerblat, B. S. *J. Phys. Chem. A* **2003**, *107*, 11102. (c) Schelter, E. J.; Prosvirin, A. V.; Reiff, W. M.; Dunbar, K. R. *Angew. Chem., Int. Ed.* **2004**, *43*, 4912. (d) Karadas, F.; Schelter, E. J.; Prosvirin, A. V.; Bacsa, J.; Dunbar, K. R. *Chem. Commun.* **2005**, 1414. (e) Schelter, E. J.; Bera, J. K.; Basca, J.; Galán-Mascarós, J. R.; Dunbar, K. R. *Inorg. Chem.* **2003**, *42*, 4256.

(11) (a) Lescouëzec, R.; Toma, L. M.; Vaissermann, J.; Verdaguer, M.; Delgado, F. S.; Ruiz-Pérez, C.; Lloret, F.; Julve, M. *Coord. Chem. Rev.* **2005**, *249*, 2691. (b) Wang, S.; Zuo, J. L.; Gao, S.; Song, Y.; Zhou, H. C.; Zhang, Y. Z.; You, X. Z. *J. Am. Chem. Soc.* **2004**, *126*, 8900. (c) Kim, J.; Han, S.; Pokhodnya, K. I.; Migliori, J. M.; Miller, J. S. *Inorg. Chem.* **2005**, *44*, 6983. (d) Li, D.; Parkin, S.; Wang, G.; Yee, G. T.; Prosvirin, A. V.; Holmes, S. M. *Inorg. Chem.* **2005**, *44*, 4903. (e) Li, D.; Parkin, S.; Wang, G.; Yee, G. T.; Holmes, S. M. *Inorg. Chem.* **2006**, *45*, 2773. (f) Li, D.; Parkin, S.; Wang, G.; Yee, G. T.; Clerac, R.; Wernsdorfer, W.; Holmes, S. M. *J. Am. Chem. Soc.* **2006**, *128*, 4214. (g) Li, D.; Parkin, S.; Wang, G.; Yee, G. T.; Holmes, S. M. *Inorg. Chem.* **2006**, *45*, 1951.

(12) Wang, S.; Zuo, J. L.; Zhou, H. C.; Choi, H. J.; Ke, Y.; Long, J. R.; You, X. Z. *Angew. Chem., Int. Ed.* **2004**, *43*, 5940.

(13) Wang, C. F.; Zuo, J. L.; Bartlett, B. M.; Song, Y.; Long, J. R.; You, X. Z. *J. Am. Chem. Soc.* **2006**, *128*, 7162.

(14) (a) Lescouëzec, R.; Vaissermann, J.; Lloret, F.; Julve, M.; Verdaguer, M. *Inorg. Chem.* **2002**, *41*, 5943. (b) Wang, S.; Zuo, J.-L.; Zhou, H.-C.; Song, Y.; Gao S.; You, X.-Z. *Eur. J. Inorg. Chem.* **2004**, 3681.

(15) (a) Reger, D. L.; Little, C. A.; Rheingold, A. L.; Sommer, R. D.; Long, G. J. *Inorg. Chim. Acta* **2001**, *316*, 65. (b) Reger, D. L.; Little, C. A.; Young, V. G., Jr.; Pink, M. *Inorg. Chem.* **2001**, *40*, 2870. (c) Galet, A.; Niel, V.; Muñoz, C.; Real, J. A. *J. Am. Chem. Soc.* **2003**, *125*, 14224. (d) Galet, A.; Muñoz, C.; Gaspar, A. B.; Real, J. A. *Inorg. Chem.* **2005**, *44*, 8749.

acetonitrile was added. The solution was filtered. Red block-shaped crystals of **1** were obtained by diffusing ether vapor into the filtrate. Yield: 80%. Anal. Calcd for $C_{68}H_{104}B_3ClFe_3N_{39}Ni_2O_{19}$: C, 38.44; H, 4.93; Fe, 7.89; N, 25.71; Ni, 5.52. Found: C, 38.47; H, 4.91; Fe, 7.45; N, 25.72; Ni, 5.87. IR (KBr, $cm^{-1}$): 2128 and 2164 ($\nu_{CN}$).

**Preparation of Complex $[(Tp)_3(Tpm^{Me})_2Co_2Fe_3(CN)_9]ClO_4\cdot 15H_2O$ (2).** An acetonitrile solution (2 mL) of $Co(ClO_4)_2\cdot 6H_2O$ (36.6 mg, 0.10 mmol) was treated dropwise by an acetonitrile solution (2 mL) of $HC(3,5\text{-}Me_2pz)_3$ (29 mg, 0.10 mmol). To this solution, $(Bu_4N)[(Tp)Fe(CN)_3]$ (88 mg, 0.15 mmol) in 3 mL of acetonitrile was added. The solution was filtered. Red block-shaped crystals of **2** were obtained by diffusing ether vapor into the filtrate. Yield: 70%. Anal. Calcd for $C_{68}H_{104}B_3ClCo_2Fe_3N_{39}O_{19}$: C, 38.43; H, 4.93; Co, 5.55; Fe, 7.88; N, 25.71. Found: C, 38.45; H, 4.90; Co, 5.86; Fe, 8.34; N, 25.73. IR (KBr, $cm^{-1}$): 2122 and 2155 ($\nu_{CN}$).

**Preparation of Complex $[(Tp)_3(Tpm^{Me})_2Fe_5(CN)_9]BF_4\cdot 15H_2O$ (3).** Solid $[Fe(Tpm^{Me})(H_2O)_3](BF_4)_2$ (54 mg, 0.10 mmol) was added to a solution of $(Bu_4N)[(Tp)Fe(CN)_3]$ (88 mg, 0.15 mmol) in 5 mL of acetonitrile. The solution was filtered. Black red block-shaped crystals of **3** were obtained by diffusing ether vapor into the filtrate. Yield: 65%. Anal. Calcd for $C_{68}H_{104}B_4F_4Fe_5N_{39}O_{15}$: C, 38.78; H, 4.98; Fe, 13.26; N, 25.94. Found: C, 39.01; H, 4.95; Fe, 13.61; N, 25.96. IR (KBr, $cm^{-1}$): 2123 and 2150 ($\nu_{CN}$).

**X-ray Structure Determination.** The crystal structures were determined on a Siemens (Bruker) SMART CCD diffractometer using monochromated Mo K$\alpha$ radiation ($\lambda$ = 0.710 73 Å) at 173 K. Cell parameters were retrieved using SMART software and refined using SAINT[16] on all observed reflections. Data were collected using a narrow-frame method with scan widths of 0.30° in $\omega$ and an exposure time of 10 s/frame. The highly redundant data sets were reduced using SAINT[16] and corrected for Lorentz and polarization effects. Absorption corrections were applied using SADABS[17] supplied by Bruker. Structures were solved by direct methods using the program SHELXL-97.[18] The positions of metal atoms and their first coordination spheres were located from direct-methods *E*-maps; other non-hydrogen atoms were found in alternating difference Fourier syntheses and least-squares refinement cycles and, during the final cycles, refined anisotropically. Hydrogen atoms were placed in calculated position and refined as riding atoms with a uniform value of $U_{iso}$. Final crystallographic data and values of $R_1$ and wR are listed in Table 1.

**Magnetic Susceptibility Measurements.** Magnetic susceptibility measurements of polycrystalline samples were measured over the temperature range 1.8−300 K with a Quantum Design MPMS-XL7 SQUID magnetometer and using an applied magnetic field from 100 to 2000 Oe. Field dependences of magnetization were measured using a flux magnetometer in the applied field up to 70 kOe generated by a conventional pulsed technique. Data were corrected for the diamagnetic contribution calculated from Pascal constants.[19] The ac measurements were performed at various frequencies from 1 to 1500 Hz with the ac field amplitude of 5 Oe and no dc field applied.

**Other Physical Measurements.** Elemental analyses for C, H, and N were performed on a Perkin-Elmer 240C analyzer. The analyses of metal ions were carried out with an inductively coupled plasma atomic emission spectrometer (ICP-AES). Mössbauer experiments were carried out using a $^{57}$Co/Pd source in a constant-acceleration transmission spectrometer. The spectra were recorded at 20 K. The spectrometer was calibrated using a standard α-Fe foil, and the reported isomer shifts ($\delta$) are relative to the center of the α-Fe spectrum. The MossWinn program was used to determine the Mössbauer parameters.[20] Infrared spectra were recorded on a Vector22 Bruker Spectrophotometer with KBr pellets in the 400−4000 $cm^{-1}$ region.

**Table 1.** Crystal and Refinement Data for Complexes **1** and **3**

| param | **1** | **3** |
|---|---|---|
| formula | $C_{68}H_{104}B_3ClFe_3N_{39}Ni_2O_{19}$ | $C_{68}H_{104}B_4F_4Fe_5N_{39}O_{15}$ |
| fw | 2124.75 | 2106.39 |
| cryst system | trigonal | trigonal |
| space group | $P\bar{3}c1$ | $P\bar{3}c1$ |
| $a$ (Å) | 17.862(7) | 18.062(2) |
| $b$ (Å) | 17.862(7) | 18.062(2) |
| $c$ (Å) | 45.776(5) | 45.948(1) |
| α (deg) | 90.00 | 90.00 |
| $\beta$ (deg) | 90.00 | 90.00 |
| $\gamma$ (deg) | 120.00 | 120.00 |
| $Z$ | 4 | 4 |
| $V$ (Å$^3$) | 12 649(2) | 12 982(4) |
| $D_{calc}$ (g $cm^{-3}$) | 1.116 | 1.078 |
| $T$ (K) | 173(2) | 173(2) |
| $\lambda$ (Å) | 0.710 73 | 0.710 73 |
| $\mu$ ($mm^{-1}$) | 0.713 | 0.609 |
| $F$(000) | 4412 | 4364 |
| $\theta$ range (deg) | 0.89−26.00 | 1.60−26.00 |
| *hkl* range | $-19 \le h \le 17$ | $-21 \le h \le 21$ |
| | $-16 \le k \le 22$ | $-22 \le k \le 20$ |
| | $-45 \le l \le 56$ | $-56 \le l \le 55$ |
| data collcd | 8305 | 8512 |
| unique data | 5355 | 5541 |
| no. of params | 463 | 460 |
| goodness of fit | 1.013 | 1.02 |
| $R_1$ ($I > 2\sigma(I)$) | 0.0251 | 0.0586 |
| $wR_2$ ($I > 2\sigma(I)$) | 0.1258 | 0.1174 |

**Table 2.** Selected Bond Lengths (Å) and Angles (deg) in Complexes **1** and **3**

| param | **1** | **3** |
|---|---|---|
| M1···Fe1 | 5.090 | 5.152 |
| M2···Fe1 | 5.131 | 5.191 |
| Fe1−C10 | 1.891(3) | 1.909(4) |
| Fe1−C11 | 1.916(4) | 1.944(3) |
| Fe1−C12 | 2.020(3) | 1.881(3) |
| M1−N7 | 2.054(2) | 2.115(3) |
| M2−N8 | 2.067(2) | 2.128(3) |
| M1−N10 | 2.155(2) | 2.236(3) |
| M2−N12 | 2.128(2) | 2.195(3) |
| Fe1−C10−N7 | 174.8(2) | 176.7(3) |
| Fe1−C11−N8 | 177.3(3) | 177.1(3) |
| Fe1−C12−N9 | 177.3(3) | 178.3(3) |
| M1−N7−C10 | 168.36(2) | 168.4(3) |
| M2−N8−C11 | 169.34(2) | 169.4(3) |
| N7−M1−N10 | 173.18(1) | 172.96(1) |
| N8−M2−N12 | 93.97(9) | 92.39(1) |

## Results and Discussion

**Structural Description.** Complexes **1** and **3** are isostructural, and relevant structural parameters are given in Table 2. The clusters crystallize in the trigonal $P\bar{3}c1$ space group, with a well-isolated $[(Tp)_3(Tpm^{Me})_2Fe_3M_2(CN)_9]^+$ cluster bearing a $C_3$ axis (M = Ni and Fe). As shown in Figures 1

(16) *SAINT-Plus*, version 6.02; Bruker Analytical X-ray System: Madison, WI, 1999.
(17) Sheldrick, G. M. *SADABS: An empirical absorption correction program*; Bruker Analytical X-ray Systems: Madison, WI, 1996.
(18) Sheldrick, G. M. *SHELXTL-97*; Universität of Göttingen: Göttingen, Germany, 1997.
(19) Wertz, J. E.; Bolton, J. R. *Electron Spin Resonance: Elementary Theory and Practical Applications*; Chapman and Hall: New York, 1986.
(20) Lencsár, Z. K.; Kuzmann, E.; Vértes, A.; Radioanal, J. *Nucl. Chem.* **1996**, *210*, 105.

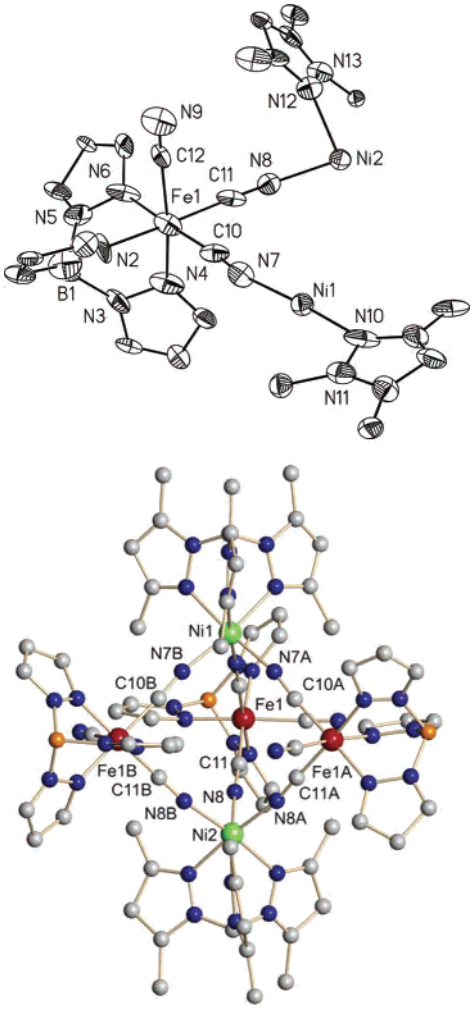


**Figure 1.** Top: Perspective drawing of the asymmetric unit of complex **1** showing the atom numbering. Thermal ellipsoids are drawn at the 50% probability levels. Bottom: Structure of the $[(Tp)_3(Tpm^{Me})_2Fe_3Ni_2(CN)_9]^+$ cluster. The hydrogen atoms and solvents are omitted for clarity.

and S1 (Supporting Information), both two clusters have the trigonal bipyramid geometry in which two octahedral $[M(Tpm^{Me})]^{2+}$ units situated in the apical positions are bridged through $CN^-$ groups to three octahedral $[(Tp)Fe(CN)_3]^-$ units that occupy the equatorial plane. Each $Fe^{III}$ ion is linked to $M^{II}$ centers through two of its three nearly linear cyanide bridges and is capped by the tridentate Tp ligand. The $Fe^{III}$−N(pyrazole) bond lengths in **1** (1.913(2)−1.953(3) Å) and **3** (1.968(3)−1.980(3) Å) are very close to those found in complexes based on poly(pyrazolyl)borates tricyanide building blocks.[11−14] Good agreement is observed between the $Fe^{III}$−C(cyano) bond lengths (1.891(3)−2.020(3) Å in **1** and 1.881(3)−1.944(3) Å in **3**) and those in low-spin tricyanoiron(III) complex $[Ph_4P][(Tp)Fe(CN)_3]$ (1.910(6)−1.929(7) Å).[14a] The $M^{II}$ ions are coordinated to tridentate $Tpm^{Me}$ as well as to the nitrogen ends of three cyanide bridges. In complex **1**, the $Ni^{II}$−N distances are between 2.128(2) and 2.155(2) Å for the $Ni^{II}$−N($Tpm^{Me}$) and between 2.054(2) and 2.067(2) Å for $Ni^{II}$−$N_{CN}$. The $Fe^{III}$−C−N bond angles are close to linear (174.8(2)−177.3(3)°), whereas $Ni^{II}$−N−C angles differ significantly from linearity (168.36(2)−169.34(2)°). In complex **3**, the average $Fe^{II}$−N($Tpm^{Me}$) bond length of 2.215 Å, which is comparable to those of high-spin-state iron(II) complexes of $[Fe(Tpm^{Me})_2](BF_4)_2$ (2.164 Å)[15b] and $[Fe(Tpm^{Me})(H_2O)_3](BF_4)_2$ (2.177 Å).[15a] The high-spin-state iron(II) in **3** is also corroborated by the average $Fe^{II}$−$N_{CN}$ distance (2.122 Å), which is in good agreement with those reported cyanide-bridged iron(II) spin-crossover complexes, such as $\{Fe(3CNpy)_2[Ag(CN)_2]\}\cdot 3/2H_2O$ ($Fe^{II}$−$N_{CN}$ = 2.133 Å)[15c] and $\{Fe(pmd)_2[Ag(CN)_2]_2$ ($Fe^{II}$−$N_{CN}$ = 2.172 Å).[15d] The key bridging pathways within both clusters are the cis-diposed M−N≡C−Fe−C≡N−M linkages. The average intramolecular $Fe^{III}\cdots M^{II}$, $Fe^{III}\cdots Fe^{III}$, and $M^{II}\cdots M^{II}$ separations are 5.111, 6.857, and 6.464 Å for **1** and 5.172, 6.953, and 6.521 Å for **3**, respectively, whereas the shortest intermolecular $Fe^{III}\cdots M^{II}$, $Fe^{III}\cdots Fe^{III}$, and $M^{II}\cdots M^{II}$ distances are 8.313, 8.750, and 10.468 Å for **1** and 8.352, 8.806, and 10.582 Å for **3**.

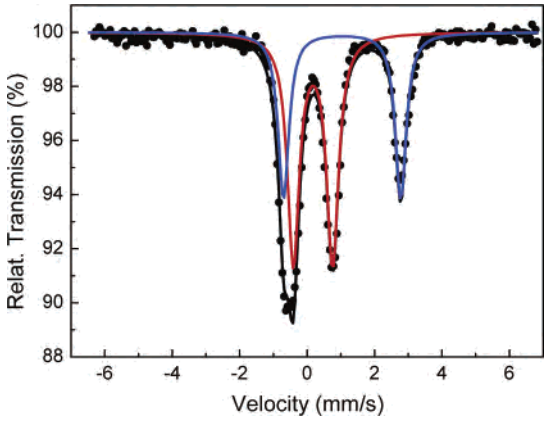


**Figure 2.** Absorption versus isomeric shift Mössbauer spectrum of **3**: experimental (●); best fit (black line); calculated absorption for $Fe^{III}$ ions (red line); calculated absorption for $Fe^{II}$ ions (blue line).

The crystal structure of complex **2** cannot be refined well because of the bad quality of the formed crystals. However, it has the same unit cell parameters and the spectroscopic data and elemental analysis results confirm that complex **2** is a pentanuclear cluster showing isomorphous structure with complexes **1** and **3**.

**Mössbauer Spectra.** The Mössbauer spectrum of **3** at $T$ = 20 K shows three absorption peaks with an isomer shift velocity of −0.628, 0.727, and 2.760 mm $s^{-1}$ (Figure 2). The experimental data can be fitted by two doublets. The first doublet possesses an isomer shift $\delta$ = 0.174(5) mm $s^{-1}$ and quadrupole spitting $\Delta E_Q$ = 1.165(6) mm $s^{-1}$, featuring characteristics of $Fe^{III}$ ions in the low-spin state in octahedral geometry. The second doublet with $\delta$ = 1.038(7) mm $s^{-1}$ and $\Delta E_Q$ = 3.475(1) mm $s^{-1}$ refers to $Fe^{II}$ ions in the high-spin state. The analysis of the band intensities leads to a $_{LS}Fe^{III}/_{HS}Fe^{II}$ ratio of 1.52, which is in good agreement with the expected value of 1.50 for $Fe^{III}_3Fe^{II}_2$ in **3**.

**Magnetic Properties.** The susceptibility variation at different temperatures of **1** was measured at 1.8−300 K (Figure 3). At room temperature, its $\chi_M T$ value is 3.23 emu K $mol^{-1}$, which is close to the spin-only value of 3.13 emu K $mol^{-1}$ expected for three low-spin $Fe^{III}$ ($S$ = 1/2) and two $Ni^{II}$ ($S$ = 1) ions in the absence of any exchange coupling. With decreasing temperature, $\chi_M T$ increases, reaching a

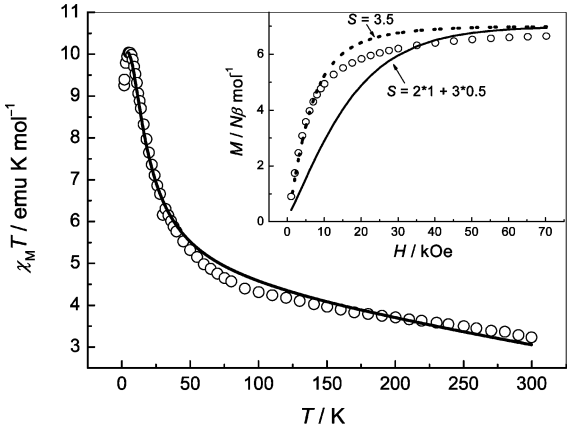


**Figure 3.** Temperature dependence of the $\chi_M T$ product for **1** at 100 Oe. Solid lines represent the best fitting of the data. The inset shows the magnetization versus the applied magnetic field at 1.8 K; the lines represents the Brillouin function that corresponds to noninteracting $S = 2S_{Ni}^{II} + 3S_{Fe}^{III}$ (solid) and $S = 3.5$ (dotted) with $g = 2.0$.

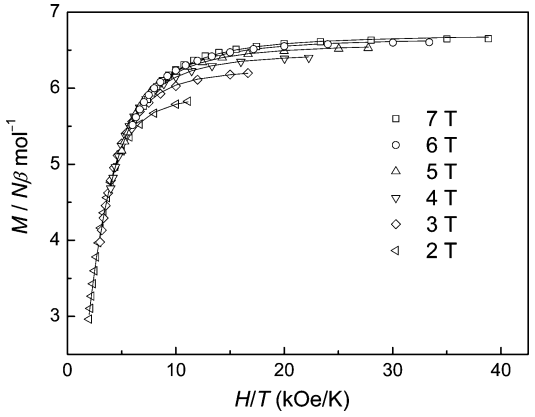


**Figure 4.** Plot of magnetization vs $H/T$ for **1** between 1.8 and 10 K. Solid lines represent a least-squares simulation of the data.

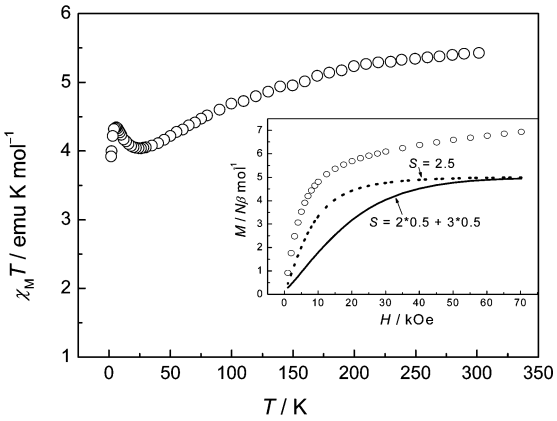


**Figure 5.** Temperature dependence of the $\chi_M T$ product for **2** at 100 Oe. The inset shows the magnetization versus the applied magnetic field at 1.8 K; the lines represents the Brillouin function that corresponds to noninteracting $S = 2S'^{II}_{Co} + 3S_{Fe}^{III}$ (solid) and $S = 2.5$ (dotted) with $g = 2.0$.

maximum of 10.07 emu K mol$^{-1}$ at approximately 5 K, suggesting ferromagnetic coupling resulted from the orthogonal spin−orbitals of the $Fe^{III}$ and $Ni^{II}$ ions. The decrease below 5 K (9.25 emu K mol$^{-1}$ at 1.8 K) could be attributed to the presence of significant zero-field splitting in the ground state. The magnetization was measured in fields up to 70 kOe, at a fixed temperature of 1.8 K, and the nearly saturated magnetization of 6.65 $N\beta$ mol$^{-1}$ at 7 T supports the $S = 7/2$ ground state for **1** (inset of Figure 3). The low-field magnetization values are fitted well with the Brillouin curve corresponding to $S = 3.5$ and higher than the Brillouin curve for noninteracting $S = 2S_{Ni} + 3S_{Fe}$ with $g = 2.0$, confirming the overall ferromagnetic $Ni^{II}$−$Fe^{III}$ interaction. The high-field magnetization values are lower than calculated, which may be due to the zero-field splitting effect. According to the structures, the exchange Hamiltonians of **1** can be described as $\mathbf{H} = -2J_1(\mathbf{S}_{Ni1} + \mathbf{S}_{Ni2})(\mathbf{S}_{Fe1} + \mathbf{S}_{Fe2} + \mathbf{S}_{Fe3}) - 2J_2(\mathbf{S}_{Fe1}\mathbf{S}_{Fe2} + \mathbf{S}_{Fe2}\mathbf{S}_{Fe3} + \mathbf{S}_{Fe3}\mathbf{S}_{Fe1}) - 2J_3\mathbf{S}_{Ni1}\mathbf{S}_{Ni2}$. Assuming $J_2 = J_3 = 0$, the best fitting results with a TIP correction were obtained from 300 to 3 K: $g = 2.27$; $J_1 = 4.84$ cm$^{-1}$; TIP $= -0.00545$.

The magnetization variation for **1** at different magnetic fields was recorded between 1.8 and 10 K (Figure 4). The nonsuperposition of the isofield lines indicates the presence of significant zero-field splitting, the effect of which results in the drop in $\chi_M T$ at very low temperature as mentioned above. With the spin ground state $S = 7/2$, fits of the magnetization data using ANISOFT[9a] for $T \leq 10$ K and $H > 1$ T afford $D = -0.79$ cm$^{-1}$ and $g = 2.12$. As we know, magnetization studies give the magnitude of the anisotropy parameters; only detailed EPR studies may give accurate values. The negative $D$ value for a $S = 7/2$ ground state reminds us that complex **1** meets one of the requirements to observe the blocking of the magnetization; i.e., it has perhaps single-molecule magnet behavior and the spin reversal barrier is $U = (S^2 - 1/4)|D| = 9.5$ cm$^{-1}$. However, ac susceptibility studies carried out in the 1.8−10 K range in a 5 Oe oscillating field at frequencies up to 1500 Hz for **1** showed no evidence for magnetic ordering or slow paramagnetic relaxation. Further magnetic measurements at lower temperature should be performed to confirm its SMMs behavior.

For **2**, the $\chi_M T$ product appears to be dominated by spin−orbit coupling effects exhibited by the cobalt(II) centers (Figure 5).[11d] At room temperature, the $\chi_M T$ value of 5.44 emu K mol$^{-1}$ is slightly higher than the expected spin-only value of 4.88 emu K mol$^{-1}$ for three low-spin $Fe^{III}$ ($S_{Fe} = 1/2$) and two high-spin $Co^{II}$ ($S_{Co} = 3/2$) ions without any exchange coupling. The $\chi_M T$ value decreases as the temperature is lowered and reaches 4.04 emu K mol$^{-1}$ at 26 K, after which point $\chi_M T$ increases to a maximum of 4.34 emu K mol$^{-1}$ at 6.0 K. Below 6 K, $\chi_M T$ drops to 3.92 emu K mol$^{-1}$ at 1.8 K. Besides the orbital contribution from $Fe^{III}$, the decrease of $\chi_M T$ value (300−26 K) may come from the orbital contribution from $Co^{II}$ and/or the depopulation of low-lying excited states. The cobalt ions can be treated with an effective spin $S'_{Co} = 1/2$ in the low-temperature range.[21] As displayed in Figure 5 (inset), the experimental values of variable-field magnetization are somewhat higher than the Brillouin curves corresponding to both $S = 2.5$ and nonin-

(21) (a) Brechin, E. K.; Cador, O.; Caneschi, A.; Cadiou, C.; Harris, S. G.; Parsous, S.; Vonci, M.; Winpenny, R. E. P. *Chem. Commun.* **2002**, 1860. (b) Plater, M. J.; Foreman, M. R. S. J.; Coronado, E.; Gómez-Garćia, C. G.; Slawin, A. M. Z. *J. Chem. Soc., Dalton Trans.* **1999**, 4209.

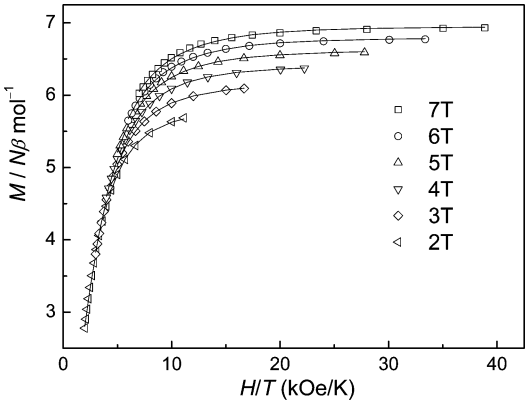


**Figure 6.** Plot of magnetization vs $H/T$ for **2** between 1.8 and 10 K. Solid lines represent a least-squares simulation of the data.

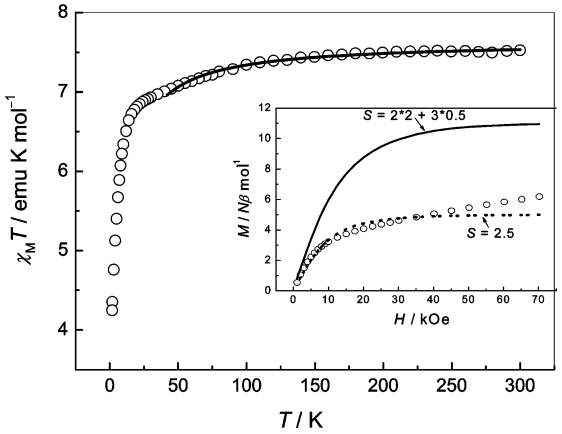


**Figure 7.** Temperature dependence of the $\chi_M T$ product for **3** at 2000 Oe. Solid lines represent the best fitting of the data. The inset shows the magnetization versus the applied magnetic field at 1.8 K; the lines represents the Brillouin function that corresponds to noninteracting $S = 2S_{Fe}^{II} + 3S_{Fe}^{III}$ (solid) and $S = 2.5$ (dotted) with $g = 2.0$.

teracting $S = 2S'_{Co} + 3S_{Fe}$ with $g = 2.0$, suggesting the overall ferromagnetic coupling between $Co^{II}$ and $Fe^{III}$ ions. The magnetization at saturation per $Fe^{III}_3Co^{II}_2$ unit is 6.93 $N\beta$ mol$^{-1}$ at 7 T (ca. 1 $N\beta$ mol$^{-1}$/$Fe^{III}$ ion ($S_{Fe} = 1/2$ and $g_{Fe} = 2$) and about 2 $N\beta$ mol$^{-1}$/$Co^{II}$ ion ($S'_{Co} = 1/2$ and $g_{Co} = 4$)), also confirming the intracluster ferromagnetic coupling existed in the cluster. However, unfortunately, the lack of an appropriate model for investigating the magnetic properties of the bimetallic low-spin $Fe^{III}$ and high-spin $Co^{II}$ centers by now impedes the evaluation of the ferromagnetic $J$ value in theory.[22]

Temperature dependence data for the magnetization of **2** were collected at a variety of fields in the temperature range of 1.8−10 K (Figure 6). With the effective spin of 1/2 for $Co^{II}$ in mind, we assume that $S = 5/2$ for complex **2**, and fits of magnetization data using ANISOFT[9a] for $T \leq 10$ K and $H > 1$ T afford zero-field splitting parameters of $D = -1.33$ cm$^{-1}$ and $g = 2.81$. On the basis of the observed values of $S$ and $D$, the spin reversal barrier energy of complex **2** should be $U = (S^2 - 1/4)|D| = 8.0$ cm$^{-1}$. However, similar to complex **1**, there is no evidence for magnetic ordering or slow paramagnetic relaxation for complex **2** from ac susceptibility studies at frequencies up to 1500 Hz.

Complex **3** shows magnetic properties different from those of complexes **1** and **2** due to their different electronic structures. The temperature dependence of susceptibility in the form of $\chi_M T$ vs $T$ at 2 kOe is shown in Figure 7. At room temperature, the $\chi_M T$ value is 7.53 emu K mol$^{-1}$, somewhat above the spin-only value of 7.13 emu K mol$^{-1}$ on the basis of three low-spin $Fe^{III}$ ($S = 1/2$) and two high-spin $Fe^{II}$ ($S = 2$) ions. Between 300 and 30 K, the $\chi_M T$ values gradually decrease from 7.53 to 6.93 emu K mol$^{-1}$ and then more abruptly below ca. 10 K, reaching a minimum value of 4.27 emu K mol$^{-1}$ at 1.8 K indicating that the $Fe^{III}$ and $Fe^{II}$ centers couple antiferromagnetically. Using an approximate isotropic model similar to that for **1**, the $\chi_M T$ value was fitted above 40 K for **3** giving $g = 2.065(1)$ and $J_1 = -0.74(4)$ cm$^{-1}$. Further evidence of antiferromagnetic coupling between the metal ions comes from the field dependence of magnetization measurements at 1.8 K, the values of which are significantly lower than the Brillouin curve corresponding to two noninteracting $S_{Fe}^{II}$ and three $S_{Fe}^{III}$ spins (inset of Figure 7).

Complexes **1**−**3** are isostructural clusters. For **1**, the orthogonality of the magnetic orbital for $Ni^{II}$ and $Fe^{III}$ ions leads to ferromagnetic interaction and the low-symmetry space group results in the overall negative molecular anisotropy ($D = -0.79$ cm$^{-1}$). We note that the location exchange of $Ni^{II}$ and $Fe^{III}$ ions, as in $\{[Ni(tmphen)_2]_3[Fe(CN)_6]_2 \cdot 14H_2O$,[23] generate a positive anisotropy. After the replacement of $Ni^{II}$ for $Co^{II}$, the zero-field splitting parameter $D$ deducted from the magnetization data is increased to −1.33 cm$^{-1}$ for **2**, which is due to the larger single-ion anisotropy for the cobalt ions. The introduction of high-spin $Fe^{II}$ in **3** leads to antiferromagnetic coupling as expected from orbital symmetry considerations.

As we know, the comparison of the $D$ values cannot be made for clusters that have different topologies and different spin states. However, it is of interest to note that the molecular symmetries show significant effects on the magnetic properties of cyano-bridged $Fe^{III}_xM^{II}_y$ clusters. The pentanuclear $Fe^{III}_3Ni^{II}_2$ (**1**) has a negative $D_{7/2}$ value of −0.79 cm$^{-1}$ as discussed above, which is larger than the value of $D = -0.23$ cm$^{-1}$ associated with the $S = 6$ ground state of $Fe^{III}_4Ni^{II}_4$ cluster crystallized in the $I4_1/acd$ space group[11f] but apparently smaller than the values of −3.89 cm$^{-1}$ associated with the $S = 3$ ground state of $Fe^{III}_2Ni^{II}_2$ clusters crystallized in the $P2_1/n$ space group.[11d] These results demonstrate the significant impact that symmetry structural distortion of the cluster core can have on magnetic anisotropy, which may lead to the enhancement of the overall anisotropy.

(22) (a) Lescouëzec, R.; Vaissermann, J.; Ruiz-Pérez, C.; Lloret, F.; Carrasco, R.; Julve, M.; Verdaguer, M.; Dromzee, Y.; Gatteschi, D.; Wernsdorfer, W. *Angew. Chem., Int. Ed.* **2003**, *42*, 1483. (b) Toma, L. M.; Lescouëzec, R.; Lloret, F.; Julve, M.; Vaissermann, J.; Verdaguer, M. *Chem. Commun.* **2003**, 1850. (c) Toma, L. M.; Lescouezec, R.; Pasan, J.; Ruiz-Perez, C.; Vaissermann, J.; Cano, J.; Carrasco, R.; Wernsdorfer, W.; Lloret, F.; Julve, M. *J. Am. Chem. Soc.* **2006**, *124*, 9336.

(23) Berlinguette, C. P.; Galán-Mascarrós, J. R.; Dunbar, K. R. *Inorg. Chem.* **2003**, *42*, 3416.

In conclusion, the strategy using complexes partially blocked by bulky organic ligand, such as $[M(Tpm^{Me})(H_2O)_3]^{2+}$ (M = Ni, Fe, Co), we used here is perhaps one of the alternative but effective approaches to prepare high-spin clusters that may exhibit SMM behavior. We are currently investigating other $M-Tpm^{Me}$ (M = Mn, Cu) building blocks with various tris(pyrazolyl)methane ligands. Moreover, we will try to introduce some other cyanometalates, such as $[M(CN)_6]^{n-}$ (M = Fe, Cr, V, Mn), into the system in place of $[Bu_4N][(Tp)Fe(CN)_3]$, to make new cyano-bridged compounds with interesting structures and magnetic properties.

**Acknowledgment.** This work was supported by the National Natural Science Foundation of China (Grant Nos. 20531040 and 90501002), the Major State Basic Research Development Program (Grant No. 2006CB806104), the Program for New Century Excellent Talents in the University of China (Grant No. NCET-04-0469), and the Natural Science Foundation of Jiangsu Province (Grant No. BK2006512). We thank the reviewers for their valuable comments and suggestions to improve the manuscript.

**Supporting Information Available:** Additional figures and X-ray crystallographic files in CIF format for **1** and **3**. This material is available free of charge via the Internet at http://pubs.acs.org.

IC060772H